IEEE Access
Multidisciplinary | Rapid Review | Open Access Journal

Received May 8, 2020, accepted July 14, 2020, date of publication July 21, 2020, date of current version July 31, 2020.

Digital Object Identifier 10.1109/ACCESS.2020.3010996

A Hybrid-Plasmonic-Waveguide-Based Polarization-Independent Directional Coupler

LI ZHANG, CAN PAN, DEZHENG ZENG, YANZHAO YANG, YATAO YANG, AND JUNXIAN MA

College of Electronics and Information Engineering, Shenzhen University, Shenzhen 518060, China

Corresponding authors: Yatao Yang (yatao86@szu.edu.cn) and Junxian Ma (majx@szu.edu.cn)

ABSTRACT In optical interconnection field, inconsistent coupling behaviors of TE and TM modes may cause abnormal operation. Therefore, it is very significant to implement a polarization-independent directional coupler. In this paper, a hybrid-plasmonic-waveguide-based polarization-independent directional coupler has been proposed. Since the energy of the hybrid plasmonic waveguides for TE and TM modes is distributed in different layers, we manage to achieve polarization independence by adjusting the material properties and dimensions of the corresponding layer. We optimize the parameters of our proposed directional coupler such as radius of silicon waveguide layer, height of silica waveguide layer, and the distance between the two waveguides, etc. Then performance of the directional coupler has been evaluated. It is worth mentioning that the length of the coupling section is only 4.25μm. Meanwhile, the polarization-dependent loss is only 0.393 dB, and the maximum coupling efficiency of TE and TM modes can reach 86.4% and 94.6%, respectively. Besides, the coupling efficiency of TM mode remains above 90% over the entire C-band, while the coupling efficiency also keeps at least 80% for TE mode. Finally, the manufacture process for the proposed directional coupler has been discussed. In brief, the improved polarization-independent directional coupler features small size, low energy loss, good polarization-independent characteristics, and wavelength insensitivity simultaneously. Compared to the other counterparts ever proposed, our proposed coupler can provide a perfect trade-off between device size and loss, which shows important potential applications in the fields of PIC and optical interconnection.

INDEX TERMS Directional coupler, polarization-independent, hybrid plasmonic waveguides, PIC, optical interconnection.

I. INTRODUCTION

Recently, optical interconnection has attracted much interest. Compared to electrical interconnection, it can better meet the requirements of data storage and transmission of communication network in the big data era [1]–[3]. As a fundamental component of sensors [4], [5], switchers [6], and modulators [7]–[9], directional coupler is also widely used in optical interconnection for its ultra-compact structure and rather low loss. However, a majority of conventional directional couplers suffer from polarization dependence. In optical interconnection field, the polarization state of the light source can be extremely indeterminate, which will lead to abnormal operation for the case of directly processing light. Therefore, a series of methods have been proposed to get a polarization-independent directional coupler [10]–[24].

There are two major approaches that enable polarization-independent directional couplers. One solution is based on polarization diversity circuits [10]–[12], the other is to design polarization-independent structure by adjusting the properties of slot waveguides [13], [14], utilizing bent directional coupler [15]–[18], or introducing sub-wavelength gratings [19], [20]. For the polarization-diversity-circuit-based solution, firstly, the multi-polarization states of the input light are divided from each other with the aid of polarization beam splitter [21], [22], thus the component can operate in single mode. Secondly, a polarization rotator is adopted to combine the two beams of polarization state light [23], [24]. Although

The associate editor coordinating the review of this manuscript and approving it for publication was Jenny Mahoney.

the structure is highly polarization-independent by processing the input light separately, complexity and big size are the main drawbacks of this scheme. For the second strategy, specific structures have been adopted to realize polarization-independence. Different polarization-independent structures have their advantages and disadvantages. Amongst them, slot-waveguide-based architecture is very simple, however, the slot sections need to be controlled precisely. Besides, bent-coupler-based architecture can achieve a rather small polarization-dependent loss, but at the cost of introducing a multi-cascade structure, which will lead to a dramatic increase in device size. Furthermore, compared to silicon-on-insulator-platform-based directional couplers, whose TM polarization intensity is much higher than TE polarization intensity, the grating-assisted structure can greatly enhance the intensity of TE polarization. Hence, both TE and TM polarization states can couple equally. For the second solution, besides the aforementioned three structures, a hybrid plasmonic waveguide (HPWG) can also help to achieve a polarization-independent directional coupler. HPWG was proposed by professor Xiang Zhang, and it has a superior trade-off between field constraint and propagation loss [25], [26]. Due to concentrating in different layers, TE and TM modes can finally get an equal polarization intensity by changing the material properties and dimensions of the corresponding layer [27]. The ultra-strong optical field constraint and the rather low propagation loss make hybrid-plasmonic-waveguide-based couplers perfectly meet the requirements of optical interconnection.

In this paper, based on our previous work [28]–[31], we propose a low loss, broadband, and polarization-independent hybrid-plasmonic waveguide directional coupler, and address its main characteristics theoretically. Using the finite element method (FEM) simulation software (FDTD solutions and COMSOL Multiphysics), we mainly focus on analyzing the effects of various material properties and dimensions on TE and TM modes, and then optimize the parameters of the polarization-independent directional coupler. The main contributions of this paper can be summarized as follows. Firstly, we demonstrate that only the radius of the cylindrical waveguide is large enough that the TE mode does not cut off. Secondly, by analyzing the field distributions of TE and TM modes, we find that the energy of the two modes is distributed in different layers, which is the crucial point to achieve polarization-independence. Then, a set of optimized parameters is obtained after studying the influence of different parameters on coupling length for TE and TM modes. Moreover, considering the conditions of weak coupling, the final optimized structure is acquired. Finally, referring to some existing structures, the characteristics of the optimized directional coupler are evaluated in terms of insertion loss, polarization-dependent loss, and wavelength sensitivity. Our hybrid-plasmonic-waveguide-based directional coupler achieves a good trade-off between device size and loss, with 4.25 μm of device length and only 0.393 dB of polarization-dependent loss.

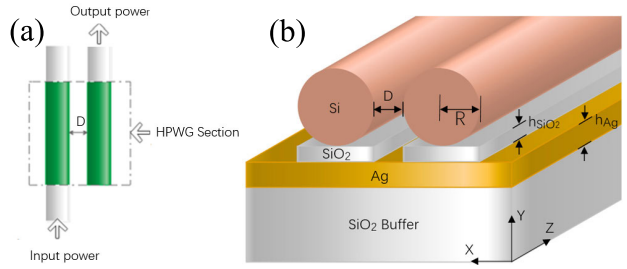

FIGURE 1. (a) The top view of the HPWG directional coupler with input and output silicon waveguides. (b) The 3D view of the coupler.

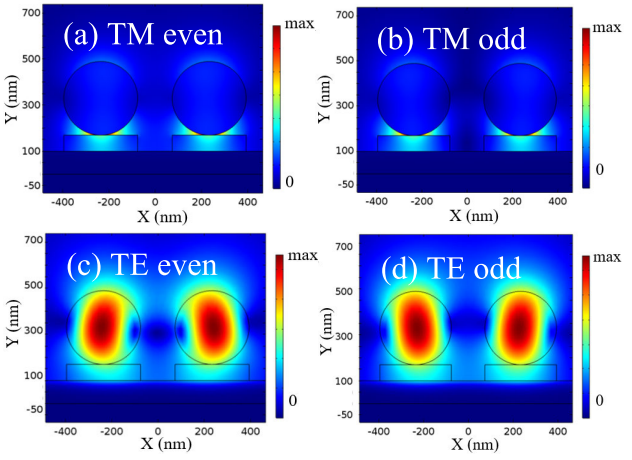

FIGURE 2. (a)–(d) Power density profiles for TM and TE modes in the coupler section (XY plane) at 1.55 μm. Device dimensions: D = 200 nm, h_{SiO_2} = 104 nm, R = 160 nm, h_{Ag} = 100 nm.

II. STRUCTURAL MODEL AND OPTIMIZATION

A. STRUCTURAL MODEL

The schematic diagram of the polarization-independent directional coupler is shown in Fig.1. It consists of two parts, one is a coupling section with hybrid plasmonic waveguides, the other is the silicon waveguides section of the input and output. Fig.1(a) shows the top view of the HPWG directional coupler with input and output silicon waveguides. The coupling section is composed of two hybrid plasmonic waveguides shown in Fig.1(b) with a distance of D. The bottom layer is a silica (SiO_2) substrate layer, covered by a silver (Ag) layer with a thickness of h_{Ag}, and the two symmetrical silica spacer layers are placed over the silver layer with a thickness of h_{SiO_2} and a width equal to the diameter of the silicon waveguides. Finally, two parallel cylindrical silicon (Si) waveguides, each with a radius of R, are placed on the silica spacer layer to form the improved polarization-independent directional coupler. Taking into consideration the attachment depth of silver reported in Ref. [32], weak coupling mechanism, and the condition of TE mode not to cut-off, we choose the basic dimensions as follows: R = 160 nm, h_{Ag} = 100 nm, h_{SiO_2} = 104 nm, and D = 200 nm. In our design, the incident light propagates in the positive direction of the z-axis at the wavelength of 1.55 μm.

Fig.2 shows the power density distributions of the odd and even modes for TE and TM modes. For TE mode,

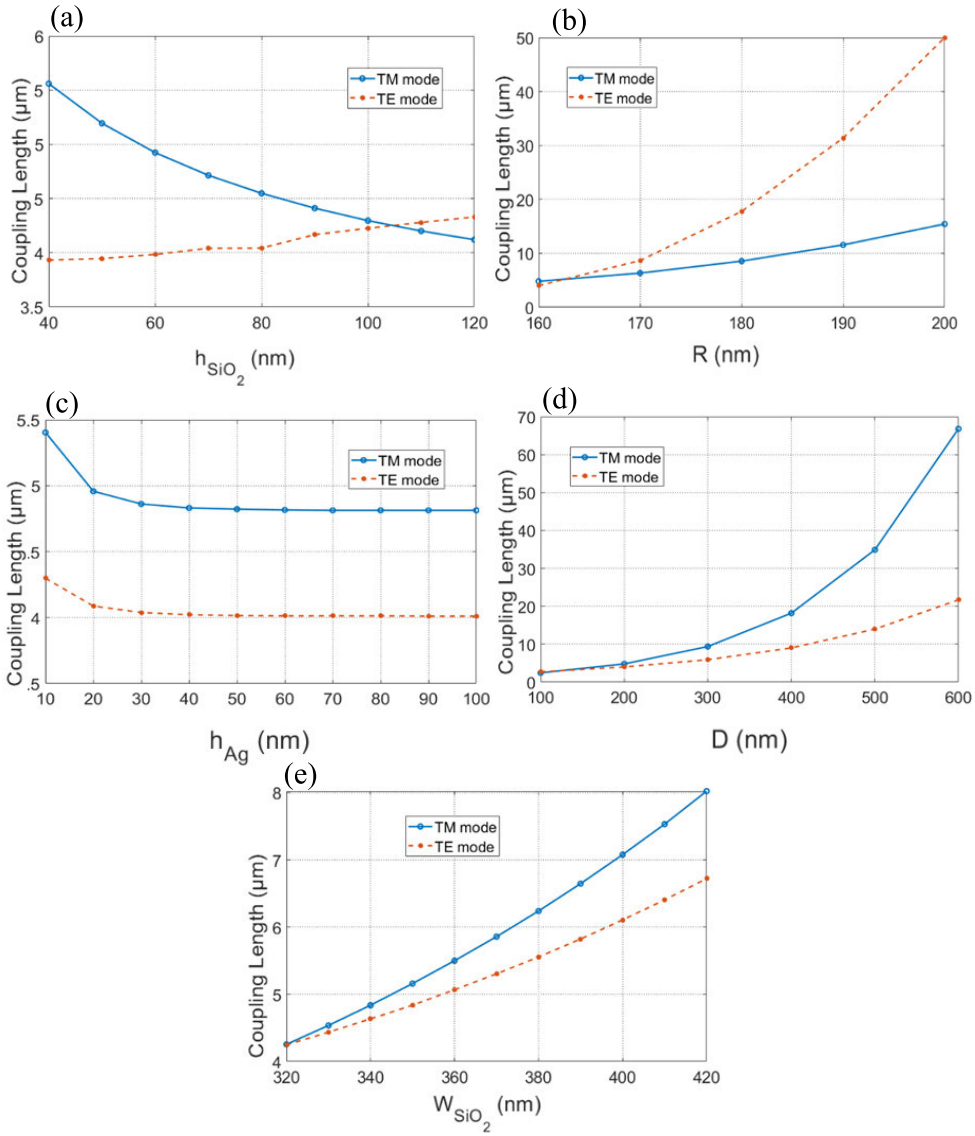

FIGURE 3. Coupling length as a function of (a) h_{SiO_2}, (b) R, (c)h_{Ag}, (d) D, (e) W_{SiO_2} with the basic dimensions: D = 200 nm, h_{SiO_2} = 65 nm, R = 160 nm, and h_{Ag} = 100 nm.

the direction of the electric field is along the y-axis, and it is along the x-axis for TM mode. When **D** is adjusted to a suitable value and the condition of the weak coupling mechanism is satisfied, the modes of the two waveguides interact and form a super mode. As can be seen from Fig.2 (a)-(d), the energy of the two polarization modes concentrates in different regions. TE mode is similar to the dielectric waveguide mode that the energy is mainly concentrated in the region of high refractive index (i.e., silicon layer). TM mode is formed by coupling between the surface plasma mode guided by the silver-silica surface and the dielectric waveguide mode guided by the silicon layer, and the energy concentrates in the gap between silica and silicon. Therefore, we can adjust the corresponding parameters to achieve a balance between TE and TM modes. Under this circumstance, the entire structure can achieve polarization independence.

B. OPTIMIZATION

We use the control variable method to analyze the effects of each parameter on TE and TM modes with a set of basic dimensions of R = 160 nm,h_{SiO_2} = 65 nm, h_{Ag} = 100 nm, and D = 200 nm. Coupling length (L_C) is the most basic characteristic of a directional coupler, which represents the distance at which the energy is completely coupled from one waveguide to the other. It is usually expressed as Eq. (1):

$$L_C = \lambda/(2\mathrm{Re}(n_{even} - n_{odd})) \tag{1}$$

where λ is the operating wavelength of 1.55 μm, n_{even} and n_{odd} are the effective mode refractive indexes of even and odd modes, respectively.

We found that TE mode, similar to the dielectric waveguide mode, will be pushed into the substrate layer and cut off if the radius of the silicon is too small. After analyzing the electric field, we got that the minimum radius is 160 nm. Fig.3

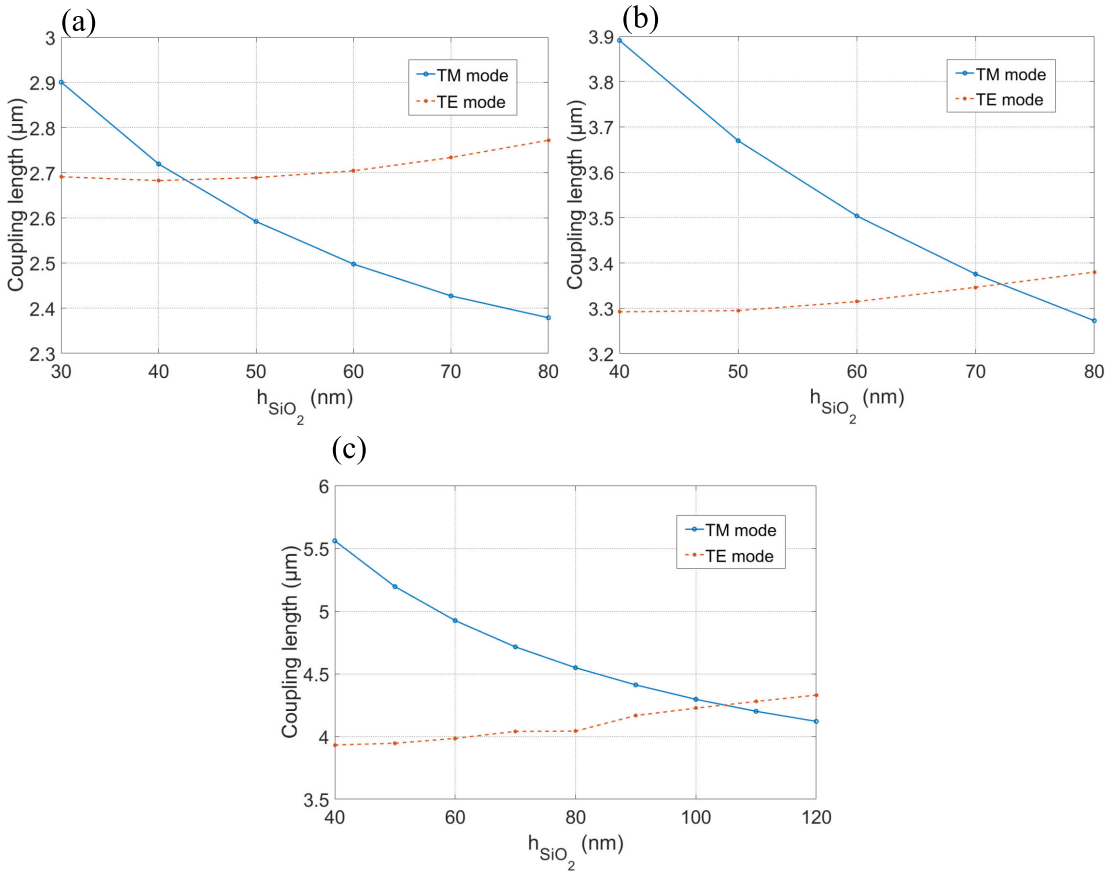

FIGURE 4. The polarization-independent cases with (a) D = 100 nm, (b) D = 150 nm, and (c) D = 200 nm.

shows the coupling length as a function of different parameters. As the optical field constraint enhances, and energy is constricted in the corresponding layer more tightly, as a consequence, the coupling length increases. From Fig.3(a), the increase of h_{SiO_2} will result in enhanced optical field constraint of TE mode and weakened optical field constraint of TM mode. Therefore, as the height of silica increases, the coupling length of TE mode increases, while that of TM mode decreases. In Fig.3(b), the increase of silicon's radius will lead to the enhanced optical field constraint of both modes, so it is reasonable that the coupling length of both TE and TM modes increases with the growth of radius. As for Fig.3(c), because of the skin depth of metal (20nm), when the thickness of Ag is less than the skin depth, it will affect the surface plasma mode formed on the surface of the silica layer. As a result, when the thickness of Ag is larger than 20 nm, the coupling length gradually becomes stable. In Fig.3(d), as the distance between the two waveguides increases, the coupling degree decreases, resulting in a growth of the coupling length. In other words, reducing distance D can improve coupling efficiency. However, when D becomes smaller, for TE mode, the light fields formed by the two waveguides are superimposed. In such circumstances, the coupling mechanism may not be satisfied, so D cannot be reduced infinitely. As can be seen from Fig.3(e), the coupling length of both modes increases slowly as the width of silica (W_{SiO_2}) increases. Therefore, we just set W_{SiO_2} equal to the diameter of the silicon waveguides.

TABLE 1. The dimensions of polarization-independent directional couplers for different values of D.

	D(nm)	h_{Sio_2}(nm)	R(nm)	h_{Ag}(nm)	L_C^{TM}(μm)	L_C^{TE}(μm)
1	100	40	160	100	2.8	2.8
2	150	70	160	100	3.35	3.35
3	200	104	160	100	4.25	4.25

From the above analysis, we can conclude that the key requirement for achieving a polarization-independent directional coupler is to vary the coupling length of both TE and TM modes in the opposite direction as the thickness of the silica increases. Fig.4 shows the polarization-independent circumstance when D is set to 100 nm, 150 nm, and 200 nm, respectively. Here, we set the basic dimensions as R = 160 nm and $h_{Ag} = 100$ nm.

Finally, the dimensions of the three polarization-independent directional couplers we obtained are listed in Table 1.

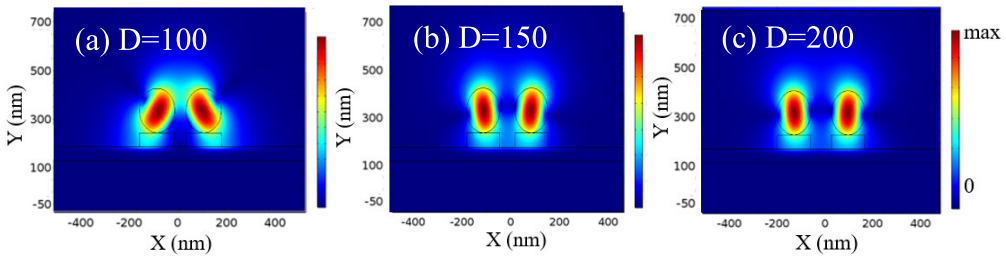

FIGURE 5. Power density profiles of TE odd mode with (a) D = 100 nm, (b) D = 150 nm, and (c) D = 200 nm.

From Fig.5, when D is equal to 100 nm or 150 nm, the odd mode of TE does not satisfy the condition of weak coupling, and the light fields formed by the two waveguides interact with each other that causes a loss of coupling energy. According to the simulation results, after a period of coupling, the coupling efficiency of TE is only 76% at D = 150 nm, while almost 86.4% at D = 200 nm. Therefore, considering the energy loss and the compactness of the structure, the third set (i.e., D = 200 nm) is the optimal dimension set for the polarization-independent directional coupler.

III. CHARACTERISTICS ANALYSIS OF THE DIRECTIONAL COUPLER

A. DEVICE PERFORMANCE

To evaluate the characteristics of the improved polarization-independent directional coupler, the polarization-dependent loss, insertion loss, and bandwidth of the structure are investigated. Besides, the normalized power and field distributions between the two waveguides are also calculated using the FEM software.

Generally, the structure of the two waveguides is the same and the power of waveguide L and R are 1 and 0 respectively when the interaction length (Z) is 0. Therefore, the power in the waveguide alternates with the transmission distance Z increases, which can be described by Eq. (2) and (3):

$$P_L(Z) = \cos^2(kZ)e^{-aZ} \tag{2}$$

$$P_R(Z) = sin^2(kZ)e^{-aZ} \tag{3}$$

where a is the exponential optical loss coefficient, and k is the coupling coefficient.

Fig.6 shows the normalized power in the input and output section for TE and TM modes as a function of the interaction length. From Fig.6, after a complete coupling period, the output power of both TE and TM modes reaches its maximum value when the interaction length is equal to 4.25 μm. For TE mode, the maximum normalized power is 0.864, and for TM mode, it is 0.946. The coupler exhibits good polarization-independent characteristics throughout the whole coupling process. This can be explained as that the output power of both modes reaches its maximum value at the end of the period of coupling. Thus, after input light source is completely coupled, no pulse broadening will occur at the output end, which leads to a great reduction in film dispersion.

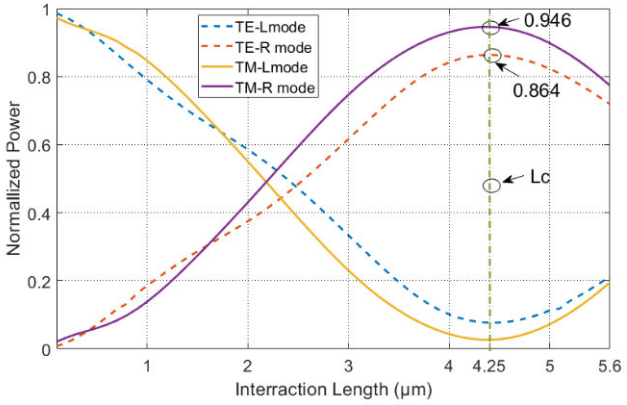

FIGURE 6. Normalized power at the ends of the input and output section as a function of the interaction length.

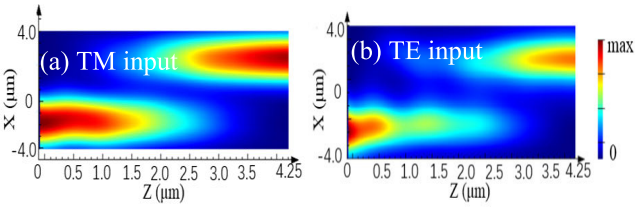

FIGURE 7. Light propagation profiles for complete coupling when the light of (a) TM and (b) TE polarization is launched.

Consequently, polarization independence is achieved. Fig.7 shows the field distributions during the coupling process. It shows that the coupling behavior of both TE and TM modes is basically the same in the whole coupling process, and the maximum value is acquired at the output end, which further verified the results obtained from Fig.6.

In order to evaluate the properties of the improved structure, polarization-dependent loss (PDL) and insertion loss (IL) of the structure are also studied, which are defined in the equations below:

$$PDL = |10\lg\left(\frac{P_{TE_{out}}}{P_{TM_{out}}}\right)|(dB) \tag{4}$$

$$IL = 10\lg\left(\frac{P_{in}}{P_{out}}\right)(dB) \tag{5}$$

Here, P_{TE_out} and P_{TM_out} represent the normalized power of TE mode and TM mode at the output port, respectively.

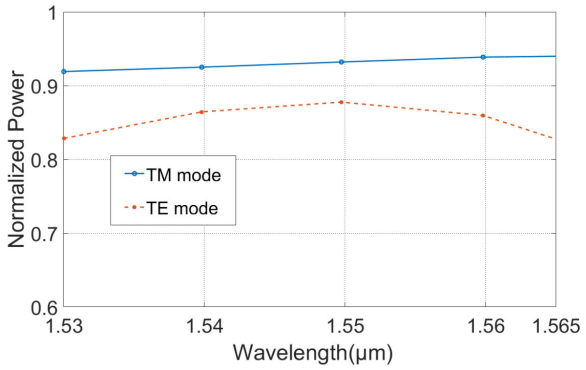

FIGURE 8. The normalized power as a function of wavelength.

TABLE 2. Characteristics of the polarization-Independent directional coupler for various structures.

Structure	Length (μm)	Energy Loss (dB)	Polarization-dependent loss (dB)
Slot waveguides[14]	8	Insertion < 0.7	/
bent waveguides[18]	Dozens	Insertion 0.315	0.05
assisted grating[20]	3.75	Excess <1	0.5
Our HPWG	4.25	Insertion<0.635	0.393

P_{in} and P_{out} denote normalized power of input port and output port, respectively.

Polarization-dependent loss describes whether the coupling behavior of both TE and TM modes is consistent. The polarization-dependent loss of our proposed coupler is only 0.393 dB, which is quite small compared to the same type of polarization-independent coupler. Insertion loss represents the energy loss during the coupling process. After

one cycle of coupling, the insertion loss of TE mode is 0.635dB, and for TM mode it is only 0.241 dB, which demonstrates that the energy loss during coupling is rather small.

Since the same structure exhibits different effective mode refractive indices at different wavelengths, it is necessary to evaluate the wavelength sensitivity of the device. As Fig.8 shows, the improved polarization-independent directional coupler has good wavelength insensitivity. Over the entire C-band (1530 nm −1565 nm), The coupling efficiency of TM mode remains above 90%, and it is also at least 80% for TE mode.

Table 2 presents a comparison of the characteristics of the polarization-independent directional couplers for various structures, and all the items are simulated results. For bent-waveguide-based directional couplers, the significant advantages are low energy loss and polarization-dependent loss. However, the big size of dozens of microns is not conducive to device integration. As for slot-waveguide-based and gratings-assisted polarization-independent directional couplers, although the size is small, the energy loss and the polarization-dependent loss are much higher compared to the bent-waveguide-based structure. Our hybrid-plasmonic-waveguide-based directional coupler combines the advantages of the other structures and provides a good balance between device size and loss. With the device length of 4.25 μm, the polarization-independent loss is only 0.393 dB, and the insertion loss for TE and TM modes is only 0.635dB and 0.241 dB, respectively.

B. FABRICATION ANALYSIS

Regarding fabrication, we analyzed the fabrication tolerance of the main parameters (i.e. h_{SiO_2} and R). Fig.9 helps to observe the details around the crossing of the TE and TM curves. Fig.9(a) shows that the normalized power varies a little with the height of silica varies between 100 nm and 110 nm, thus it has little impact on the device's performance. Fig.9(b) depicts the normalized power variation with the radius of silicon varies between 160 nm and 170 nm. For TE mode, the performance of the device is very sensitive

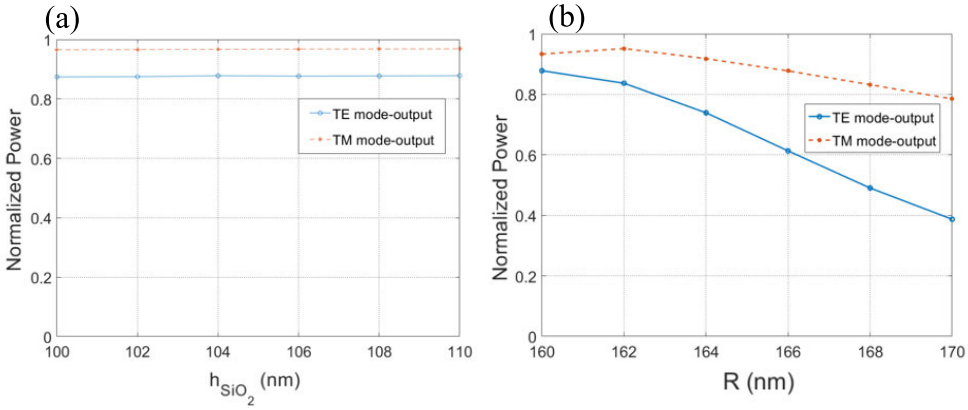

FIGURE 9. Normalized power variation with (a) h_{SiO_2} = 100∼110nm, (b) R = 160∼170 nm.

to the radius of silicon. It indicates that the fabrication tolerance is small in terms of the radius of silicon. This is the common problem that hybrid-plasmonic-waveguide-based devices have. So, fabrication tolerance is indeed one of the challenges that hybrid plasmonic waveguide has to face. However, many of the ever proposed hybrid plasmonic waveguide and relevant hybrid-plasmonic-waveguide-based devices like directional coupler, have been fabricated successfully in the laboratory [21], [33]–[35].

According to our design, we referred literature [21], [33]–[36], and discussed with some researchers from Micro-nano laboratories, then confirmed the corresponding fabrication process for our proposed directional coupler. The main process can be as follows: first, a silver layer with a thickness of h_{Ag} is evaporated on top of a 3 μm thick SiO_2 buffer layer by electron beam evaporation. Then, a thin SiO_2 film of thickness h_{SiO_2} is deposited by plasma-enhanced chemical vapor deposition using in-house optimized technology. After that, patterns are generated by e-beam lithography (Raith 150 at 25 kV) using negative resist ma-N 2403. Because the silicon layer uses a cylindrical nanowire waveguide, it is a little difficult to fabricate using photolithography technology. Finally, we decide to transfer the pre-grown cylindrical silicon waveguide by transfer printing, and then use the Nanoprobe to lay out the position and shape.

IV. CONCLUSION

In summary, we proposed a hybrid-plasmonic-waveguide-based polarization-independent directional coupler and evaluated its characteristics by using FEM software. Through the field distribution analysis, we found that TE and TM modes have different energy distribution regions, which indicates that we can achieve polarization independence by adjusting the material properties and dimensions of the corresponding layer. Besides, by studying the influences of each parameter on TE and TM modes, a set of optimized parameters is obtained. Moreover, taking into account the condition of weak coupling, the final optimized parameters are obtained. Usually, there are trade-offs among energy loss, polarization-dependent loss, and device size when designing a directional coupler, and our optimized coupler can achieve a perfect trade-off. With the small coupling section length of 4.25μm, the polarization-dependent loss is only 0.393 dB, and the maximum coupling efficiency of TE and TM modes can reach 86.4% and 94.6%, respectively. Besides, the structure exhibits superior wavelength insensitivity in C-band. Specifically, the coupling efficiency of TM mode remains above 90%, and also keeps above 80% for TE mode. Additionally, concerning manufacture, we discuss fabrication tolerance, and provide the most probable manufacture process of the proposed directional coupler. In short, the proposed hybrid-plasmonic-waveguide-based directional coupler features small size, low energy loss, good wavelength insensitivity, and good polarization-independent characteristics. These advantages are of great importance for relevant applications in the fields of PIC and optical interconnection.

REFERENCES

[1] Y. Vlasov, "Silicon CMOS-integrated nano-photonics for computer and data communications beyond 100 G," *IEEE Commun. Mag.*, vol. 50, no. 2, pp. s67–s72, Feb. 2012.
[2] H. J. Caulfield and S. Dolev, "Why future supercomputing requires optics," *Nature Photon.*, vol. 4, no. 5, pp. 261–263, May 2010.
[3] D. Miller, "Device requirements for optical interconnects to silicon chips," *Proc. IEEE*, vol. 97, no. 7, pp. 1166–1185, Jul. 2009.
[4] H. Chen, Z. Shao, X. Zhang, Y. Hao, and Q. Rong, "Highly sensitive magnetic field sensor using tapered Mach–Zehnder interferometer," *Opt. Lasers Eng.*, vol. 107, pp. 78–82, Aug. 2018.
[5] R. W. Huggins, G. L. Abbas, C. S. Hong, G. E. Miller, C. R. Porter, and B. Vandeventer, "Fiber coupledposition sensors for aerospace applications," *Opt. Lasers Eng.*, vol. 16, nos. 2–3, pp. 79–103, 1992.
[6] D. Perron, M. Wu, C. Horvath, D. Bachman, and V. Van, "All-plasmonic switching based on thermal nonlinearity in a polymer plasmonic microring resonator," *Opt. Lett.*, vol. 36, no. 14, pp. 2731–2733, Jul. 15 2011.
[7] X. Sun, L. Zhou, Z. Hong, J. Chen, and X. Li, "Design and analysis of a phase modulator based on a metal-polymer-silicon hybrid plasmonic waveguide," *Appl. Opt.*, vol. 50, no. 20, pp. 3428–3434, 2011.
[8] S. Zhu, G. Q. Lo, and D. L. Kwong, "Theoretical investigation of silicon MOS-type plasmonic slot waveguide based MZI modulators," *Opt. Express*, vol. 18, no. 26, pp. 27802–27819, Dec. 20 2010.
[9] V. J. Sorger, N. D. Lanzillotti-Kimura, R.-M. Ma, and X. Zhang, "Ultra-compact silicon nanophotonic modulator with broadband response," *Nanophotonics*, vol. 1, no. 1, pp. 17–22, Jul. 2012.
[10] S.-H. Kim, K. Tanizawa, Y. Shoji, G. Cong, K. Suzuki, K. Ikeda, H. Ishikawa, S. Namiki, and H. Kawashima, "Compact 2×2 polarization-diversity Si-wire switch," *Opt. Express*, vol. 22, no. 24, pp. 29818–29826, Dec. 2014.
[11] Y. Ma, Y. Liu, H. Guan, A. Gazman, Q. Li, R. Ding, Y. Li, K. Bergman, T. Baehr-Jones, and M. Hochberg, "Symmetrical polarization splitter/rotator design and application in a polarization insensitive WDM receiver," *Opt. Express*, vol. 23, no. 12, pp. 16052–16062, Jun. 2015.
[12] H. Xu, L. Liu, and Y. Shi, "Polarization-insensitive four-channel coarse wavelength-division (de)multiplexer based on Mach-Zehnder interferometers with bent directional couplers and polarization rotators," *Opt. Lett.*, vol. 43, no. 7, pp. 1483–1486, Apr. 2018.
[13] T. Fujisawa and M. Koshiba, "Polarization-independent optical directional coupler based on slot waveguides," *Opt. Lett.*, vol. 31, pp. 56–58, Jan. 2006.
[14] L.-M. Chang, L. Liu, Y.-H. Gong, M.-Q. Tan, Y.-D. Yu, and Z.-Y. Li, "Polarization-independent directional coupler and polarization beam splitter based on asymmetric cross-slot waveguides," *Appl. Opt.*, vol. 57, no. 4, pp. 678–683, Feb 1 2018.
[15] X. Chen, W. Liu, Y. Zhang, and Y. Shi, "Polarization-insensitive broadband 2×23 dB power splitter based on silicon-bent directional couplers," *Opt. Lett.*, vol. 42, no. 19, pp. 3738–3740, Oct. 2017.
[16] D. Xiuling, Y. Lianshan, J. Hengyun, P. Wei, L. Bin, and Z. Xihua, "Polarization-insensitive and broadband optical power splitter with a tunable power splitting ratio," *IEEE Photon. J.*, vol. 9, no. 3, Jun. 2017, Art. no. 4501609.
[17] Y. Wang, L. Xu, H. Yun, M. Ma, A. Kumar, E. El-Fiky, R. Li, N. Abadiacalvo, L. Chrostowski, N. A. F. Jaeger, and D. V. Plant, "Polarization-independent mode-evolution-based coupler for the silicon-on-insulator platform," *IEEE Photon. J.*, vol. 10, no. 3, pp. 1–10, Jun. 2018.
[18] X. Deng, L. Yan, H. Jiang, X. Feng, W. Pan, and B. Luo, "Polarization-insensitive and tunable silicon Mach–Zehnder wavelength filters with flat transmission passband," *IEEE Photon. J.*, vol. 10, no. 3, pp. 1–7, Jun. 2018.
[19] L. Liu, Q. Deng, and Z. Zhou, "Subwavelength-grating-assisted broadband polarization-independent directional coupler," *Opt. Lett.*, vol. 41, no. 7, pp. 1648–1651, Apr. 2016.
[20] H. Xu and Y. Shi, "Ultra-compact polarization-independent directional couplers utilizing a subwavelength structure," *Opt. Lett.*, vol. 42, no. 24, pp. 5202–5205, Dec. 2017.
[21] X. Sun, M. Z. Alam, S. J. Wagner, J. S. Aitchison, and M. Mojahedi, "Experimental demonstration of a hybrid plasmonic transverse electric pass polarizer for a silicon-on-insulator platform," *Opt. Lett.*, vol. 37, no. 23, pp. 4814–4816, Dec. 2012.
[22] H. Wu and D. Dai, "High-performance polarizing beam splitters based on cascaded bent directional couplers," *IEEE Photon. Technol. Lett.*, vol. 29, no. 5, pp. 474–477, Mar. 1, 2017.

[23] J. N. Caspers, M. Z. Alam, and M. Mojahedi, "Compact hybrid plasmonic polarization rotator," *Opt. Lett.*, vol. 37, no. 22, pp. 4615–4617, Nov. 2012.
[24] A. Rostamian, J. Guo, S. Chakravarty, H. Yan, C.-J. Chung, E. Heidari, and R. T. Chen, "Grating-coupled Silicon-on-Sapphire polarization rotator operating at mid-infrared wavelengths," *IEEE Photon. Technol. Lett.*, vol. 31, no. 5, pp. 401–404, Mar. 1, 2019.
[25] R. F. Oulton, V. J. Sorger, D. A. Genov, D. F. P. Pile, and X. Zhang, "A hybrid plasmonic waveguide for subwavelength confinement and long-range propagation," *Nature Photon.*, vol. 2, no. 8, pp. 496–500, Aug. 2008.
[26] R. F. Oulton, G. Bartal, D. F. P. Pile, and X. Zhang, "Confinement and propagation characteristics of subwavelength plasmonic modes," *New J. Phys.*, vol. 10, no. 10, Oct. 2008, Art. no. 105018.
[27] M. Z. Alam, J. S. Aitchison, and M. Mojahedi, "Polarization-independent hybrid plasmonic coupler for a silicon on insulator platform," *Opt. Lett.*, vol. 37, no. 16, pp. 3417–3419, Aug. 2012.
[28] M. Zhang and J. Ma, "Transmission characteristics analysis of a hybrid SNIMS plasmonic waveguide," in *Proc. 7th Int. Symp. Adv. Opt. Manuf. Test. Technol., Design, Manuf., Test. Micro-Nano-Opt. Devices Syst.*, Aug. 2014, Art. no. 92830A.
[29] L. Zhang, Q. Xiong, X. Li, and J. Ma, "Elliptic cylindrical silicon nanowire hybrid surface plasmon polariton waveguide," *Appl. Opt.*, vol. 54, no. 23, pp. 7037–7044, Aug. 10 2015.
[30] D. Zeng, L. Zhang, Q. Xiong, and J. Ma, "Directional coupler based on an elliptic cylindrical nanowire hybrid plasmonic waveguide," *Appl. Opt.*, vol. 57, no. 16, pp. 4701–4706, Jun 1 2018.
[31] J. Ma, D. Zeng, Y. Yang, C. Pan, L. Zhang, and H. Xu, "A review of crosstalk research for plasmonic waveguides," *Opto-Electron. Adv.*, vol. 2, no. 4, 2019, Art. no. 180022.
[32] J. A. Dionne, L. A. Sweatlock, H. A. Atwater, and A. Polman, "Planar metal plasmon waveguides: Frequency-dependent dispersion, propagation, localization, and loss beyond the free electron model," *Phys. Rev. B, Condens. Matter*, vol. 72, no. 7, Aug. 2005, Art. no. 075405.
[33] F. Lou, Z. Wang, D. Dai, L. Thylen, and L. Wosinski, "Experimental demonstration of ultra-compact directional couplers based on silicon hybrid plasmonic waveguides," *Appl. Phys. Lett.*, vol. 100, no. 24, Jun. 2012, Art. no. 241105.
[34] J. N. Caspers, J. S. Aitchison, and M. Mo, "Experimental demonstration of an integrated hybrid plasmonic polarization rotator," *Opt. Lett.*, vol. 38, no. 20, pp. 4054–4057, 2013.
[35] X. Guan, P. Xu, Y. Shi, and D. Dai, "Ultra-compact broadband TM-pass polarizer using a silicon hybrid plasmonic waveguide grating," in *Proc. Asia Commun. Photon. Conf.*, 2013, p. ATh4A-2.
[36] X. Wu, S. Yu, H. Yang, W. Li, X. Liu, and L. Tong, "Effective transfer of micron-size graphene to microfibers for photonic applications," *Carbon*, vol. 96, pp. 1114–1119, Jan. 2016.

LI ZHANG received the M.S. degree in communication and information systems from Lanzhou University, China, in 1999, and the Ph.D. degree in optical engineering from the Huazhong University of Science and Technology, China, in 2008. Since 2008, she has been working with Shenzhen University. From 2016 to 2017, she worked as a Visiting Scholar with the Department of Electrical and Computer Engineering, University of California, San Diego, for a period of one year. She is currently an Associate Professor with the College of Electronics and Information Engineering, Shenzhen University. Her current research interests include optical communication and surface plasmon polariton (SPP) waveguides and devices.

CAN PAN receive the B.S. degree from Huangshan University, China, in 2018. He is currently pursuing the M.S. degree with Shenzhen University. His research interests include optical communication devices and the optical Internet of Things.

DEZHENG ZENG received the M.S. degree from Shenzhen University, China, in 2019. His research interest includes optical communication devices.

YANZHAO YANG received the B.S. degree from Shenzhen University, China, in 2018. He is currently a Laboratory Assistant with the College of Electronics and Information Engineering, Shenzhen University. His research interests include optical data transmission, data processing, and the optical Internet of Things.

YATAO YANG received the B.Sc. degree in optical instrumentation engineering from Zhejiang University, China, and the Ph.D. degree in fiber optics from Glasgow Caledonia University, U.K. He joined Institute of Optics and Electronics, Chinese Academy of Sciences, where he was involved in semiconductor equipment and optoelectronic device development. He was a Research Officer with the University of Leeds, U.K., in 1996, involved in areas of optical fiber laser materials. He joined Resonance Ltd., Canada, in 1997, where he was developing spectral gas sensors. He joined JDSU Corporation, Canada, in 1998, where he was developing optical fiber devices. He joined Chorum Technologies Inc., USA, in 2000, where he was developing optical fiber devices. He joined JDSU Corporation, USA, in 2004, where he was developing optical fiber devices and fiber lasers. He joined NeoPhotonics Corporation, as VP of Research and Development, in 2009, developing optical fiber devices. He founded Shenzhen Dade Laser Technology Co., Ltd., in 2014. He was appointed as a Distinguished Professor with the College of Electronics and Information Engineering, Shenzhen University, China, in 2017. He became the Head of the Smart IoT Center, Shenzhen University, in 2018. His research interests include optical networking, optical sensors, optical data transmission and data processing, optical nanomaterials, optical-wireless communications, and lasers.

JUNXIAN MA received the Ph.D. degree in optical engineering from the Chinese Academy of Science, in 2003. He is currently the Board Chairman of the Shenzhen Institute of Communications. He is also a tenured Professor with the College of Electronics and Information Engineering, Shenzhen University. His research interests include micro and nano components of optical fiber communication and sensor networks.